Colloid Polym Sci 273:959–966 (1995)

ORIGINAL CONTRIBUTION

P.C. Schulz
M.A. Morini
R.M. Minardi
J.E. Puig

The aggregation in dodecyltrimethylammonium hydroxide aqueous solutions

Received: 30 January 1995
Accepted: 8 May 1995

Dr. P.C. Schulz (✉) · M.A. Morini
R.M. Minardi
Department of Chemistry and
Chemical Engineering
Universidad Nacional del Sur
8000 Bahia Blanca, Argentina

J.E. Puig
Faculty of Chemical Sciences
Universidad de Guadalajara
Guadalajara, Mexico

Abstract The aggregation of dodecyltrimethylammonium hydroxide (DTAOH) aqueous solutions has been studied by several methods. It is stepwise and four critical points were found. At $C_T = (2.51 \pm 0.10) \times 10^{-4}$ mol·dm^{-3} the surface excess becomes zero, at $C_T = (1.300 \pm 0.041) \times 10^{-3}$ mol·dm^{-3} small aggregates form, which grow with concentration. At $C_T = (1.108 \pm 0.010) \times 10^{-2}$ mol·dm^{-3} true micelles form (CMC) and at $(3.02 \pm 0.28) \times 10^{-2}$ mol·dm^{-3} the structure of micelles probably changes affecting their properties. The DTAOH micelles are highly ionized ($\alpha = 0.8$) at the CMC, and decreases to reach very small values when the total concentration increases.

Key words Hydroxide surfactants – critical micelle concentration – aggregation – cationic surfactants – micelle charge

Introduction

Knowledge of the properties of hydroxide surfactants is of great interest in the theoretical interpretation of micellar catalysis [1, 2] and other phenomena as the origin of the discrepancies when alkyltrimethylammonium bromides critical micelle concentrations (CMC) are determined with bromide and with alkyltrimethylammonium (RTA$^+$) ion-selective electrodes.

There are discrepancies in the literature about the CMC of the alkyltrimethylammonium hydroxides (RTAOH). Lianos and Zana [3] found the hexadecyltrimethylammonium hydroxide (CTAOH) CMC = 1.8×10^{-3} mol·dm^{-3}, whereas other authors [4, 5] found 7.7×10^{-4} mol·dm^{-3}. The CTAB CMC is 9×10^{-4} mol·dm^{-3} [6–8]. For dodecyltrimethylammonium hydroxide (DTAOH) Lianos and Zana [3] found the CMC = $(3.05 \pm 0.30) \times 10^{-2}$ mol·dm^{-3} by conductivity measurements, and $(2.95 \pm 0.20) \times 10^{-2}$ mol·dm^{-3} by pH measurements. However, surface tension measurements give much smaller values [9]. DTAB CMC ranges from 0.011 mol·dm^{-3} [6] with DTA$^+$-ion selective electrode to 0.0175 mol·dm^{-3} [11]. Other DTAB CMC's values are 0.014 mol·dm^{-3} [6], 0.0154 mol·dm^{-3} [11] and 0.0146 mol·dm^{-3} [12].

Since the determined CMC values for RTAOH differ significantly from each other depending on the measurement method, in this work the DTAOH aggregation was studied by methods that measure properties of the system as a whole (conductivity), properties mainly depending on the single-dissolved species activity (surface tension, DTA$^+$ ion-selective electrode, pH electrode) and on the micelles (solubilization, density, viscosity). The goal was to elucidate the origin of the literature discrepancies.

Experimental

Preparation of the hydroxile surfactant

Much care was taken to avoid contamination with atmospheric CO_2 in this work. Surfactant solutions preparation and measurements were performed in a plastic sealed chamber which had several dishes with concentrated NaOH solution inside. This chamber had two plastic gloves to work inside. After introduction of the material, a flow of N_2 was passed, which previously bubbled through NaOH solution. All work inside the chamber started 2 h after the chamber was closed and nitrogen passed in. All runs were performed at 25.0 ± 0.1 °C, by water circulation from a thermostat.

The water employed was double-distilled, boiled 1 h to expel dissolved CO_2 and left to cool in a N_2 atmosphere.

A concentrated DTAOH solution was prepared by passing DTAB solution through an ion-exchange column. This column was prepared in a 50 mL burette filled by Amberlite IRA-400 (OH) (Carlo Erba). The total elimination of Br^- was verified with a $AgNO_3 + HNO_3$ solution. The whole system was sealed to avoid CO_2 contamination.

The final DTAOH concentration was determined three times by conductimetric titration with HCl.

All runs were performed in duplicate.

Surface tension measurements

The surface tension measurements were performed with a Du Nöuy (Krüss) tensiometer, which was put into the chamber. It took 1 h to stabilize the surface tension (σ) of the more dilute solutions. When the CMC was reached, the surface tension stabilized in less than 2 min.

DTA^+ ion-selective measurements

The DTA^+ ion-selective electrode was made by dissolving 0.3 g of carrier (dodecyltrimethylammonium dodecylsulphate) and 0.06 of dibutylphthalate (plastizicer) in 10 mL of tetrahydrofuran. 0.3 g of PVC were added, and the solution was let to evaporate in a Petri dish, covered by a filter paper. The elastic film obtained was glued to a PVC tube with tetrahydrofuran. The inner electrode was Ag/AgCl, and the tube was filled with NaBr 0.001 $mol \cdot dm^{-3}$ + LTAB 0.001 $mol \cdot dm^{-3}$ solution. All measurements were performed against a calomel saturated electrode and a Tacussel millivoltmeter.

The carrier was prepared by mixing equimolar quantities of DTAB and SDS solutions. Then the precipitate was filtered, washed until no Br^- was detected, and dried.

The electrode was checked by measurements on DTAB solutions, giving results which were in agreement with the literature [6].

Glass electrode measurements

OH^- determinations were made with an Orion glass electrode and pH-meter.

Computations based on electrode data

The activity coefficients γ were computed using the Davies' equation [13]:

$$\log \gamma = -0.5115\sqrt{I}/(1+\sqrt{I}) - 0.15I\,, \tag{1}$$

where I is the ionic strength. Only the unmicellized ions were considered to compute I. The unmicellized amphiphilic ion (DTA^+) and counterion (OH^-) concentrations, and the micellized material concentration (M) (on a momomeric basis) were computed from the E vs. C_T curves by literature methods [14]. Then, the effective charge per micellized surfactant molecule, $\alpha = 1 - m/n$, was computed, where m/n is the OH^- to DTA^+ ratio in the micelles:

$$m/n = \frac{C_T - [OH^-]}{C_T - [DTA^+]} \tag{2}$$

Conductivity measurements

Conductivity measurements were performed with an immersion cell and an automatic conductimeter, namely an Antares II from Instrumentalia.

Dye solubilization measurements

Sealed tubes with Sudan III or Sudan Black B and DTAOH and DTAOH solutions of different concentration were left for a week in a constant temperature bath, with periodic stirring. Then the tubes were centrifuged and the supernatant absorbance was measured with a Spectronic-20 UV-Vis spectrophotometer at 488 nm (Sudan III) or 600 nm (Sudan Black B).

Modification of dye color and fluorescence

A series of tubes was prepared and in each one DTAOH solution of different concentration and a drop of Rhodamine 6G solution were poured to detect micelle formation [15–18].

This dye showed differences in color and fluorescence between micellar and non-micellar solutions, similar to that shown by Sky Blue FF [15].

Viscosity measurements

A constant temperature Ostwald viscometer was employed, using double-distilled water as a reference substance.

Density measurements

The density measurements were performed at 20 °C with a Chainomatic density balance, using double-distilled water as a reference substance.

Computations

When straight lines were obtained, they were treated with the least squares method. Averages were obtained with the minimum variance linear unbiased estimation method [19]. A confidence level of 0.90 and Students **t** distribution function were employed in all error estimations.

Results

Figure 1 shows the DTA^+ ion-selective electrode results. The aggregation of surfactant ions occurs at $(1.3 \pm 0.1) \times 10^{-3}$ mol·dm^{-3}.

Figure 2 shows the glass electrode results. The aggregation of OH^- ions onto DTA^+ aggregates occurs at $C_T = (1.20 \pm 0.01) \times 10^{-2}$ mol·L^{-1}. As in other RTAX, the break in the DTA^+ ion-selective electrode curve occurs at a concentration less than that of the counterion [6].

Figure 3 shows the unaggregated surfactant ion (DTA^+) and counterion (OH^-) concentration and aggregated surfactant concentration (M) (on a monomer basis) as a function of C_T. The charge per micellized surfactant monomer α was plotted in Fig. 4 vs. C_T. It may be seen that DTAOH aggregates are first strongly ionized, but the charge diminishes as the total concentration increases.

From the surface tension results plotted in Fig. 5, four linear zones can be seen, whose equations are:

line I:

$$\sigma(mN/m) = -37.5 \pm 1.4 - (21.31 \pm 0.31)\log C_T$$

$$r = -0.9932$$

line II:

$$\sigma(mN/m) = 40.04 \pm 0.95 + (0.38 \pm 0.35)\log C_T$$

$$r = 0.1384$$

line III:

$$\sigma(mN/m) = 81.1 \pm 3.0 + (20.7 \pm 1.9)\log C_T$$

$$r = 0.9551$$

line IV:

$$\sigma(mN/m) = 49.66 \pm 0.54 + (0.39 \pm 0.50)\log C_T$$

$$r = 0.2046$$

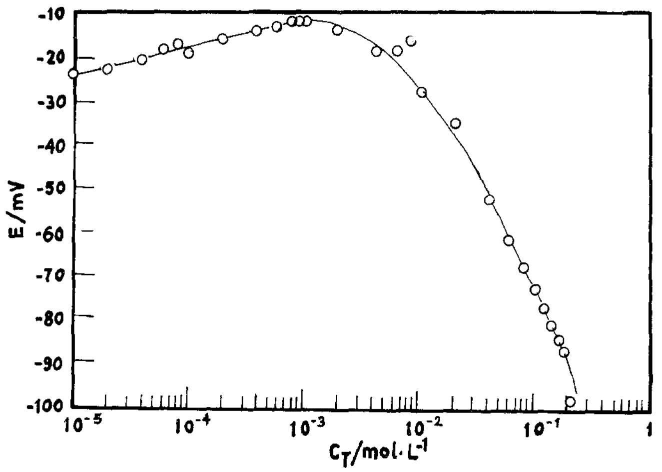

Fig. 1 DTA^+ ion-selective electrode potential vs. saturated calomel electrode, as a function of the concentration of DTAOH

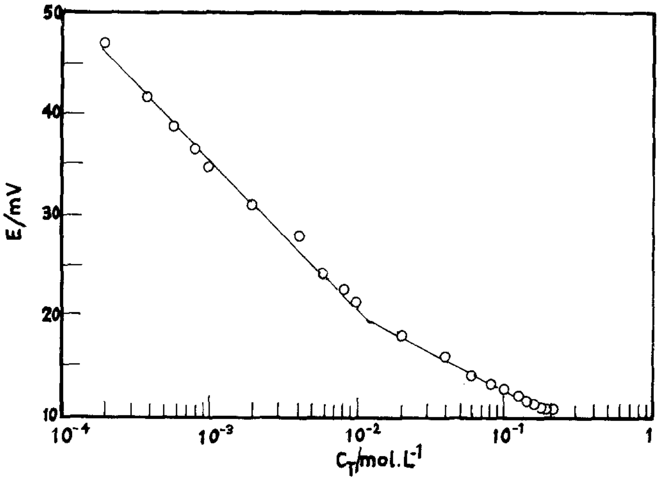

Fig. 2 Glass electrode potential vs concentration of DTAOH

Fig. 3 Concentration of: ■ unaggregated DTA^+ ions, △ unaggregated OH^- ions and ○ aggregates (on a monomeric basis) vs. the logarithm of the concentration of DTAOH

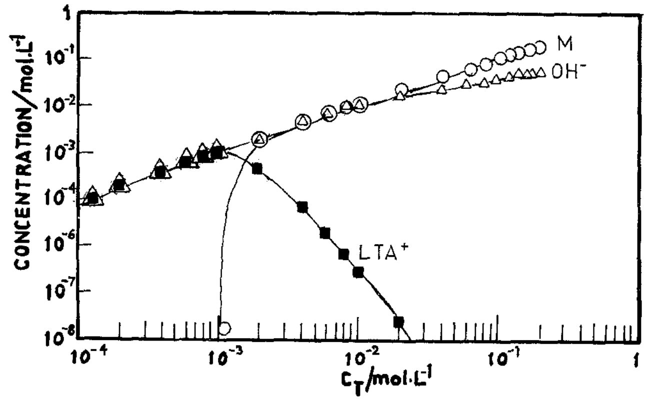

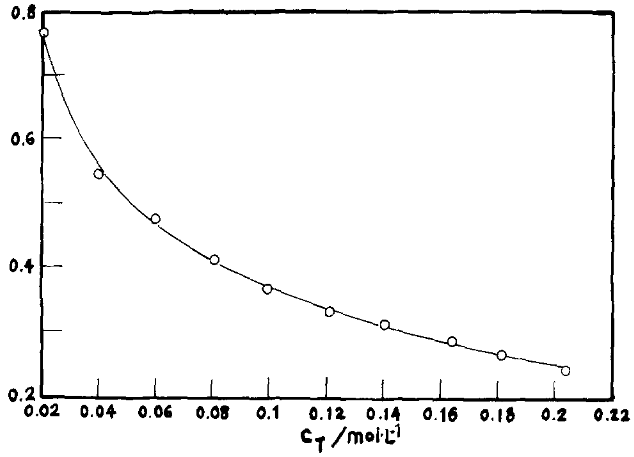

Fig. 4 The fraction of charge, α, per micellized surfactant molecule, as a function of the concentration of DTAOH

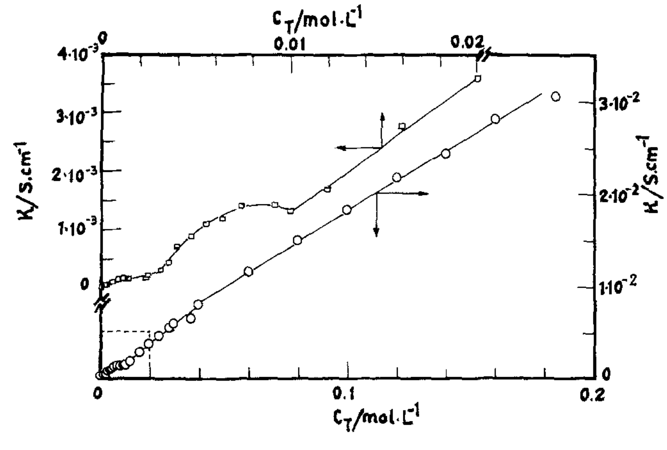

Fig. 6 The specific conductivity of DTAOH solutions vs. total concentration. The upper curve is an amplification of the small square at low concentration

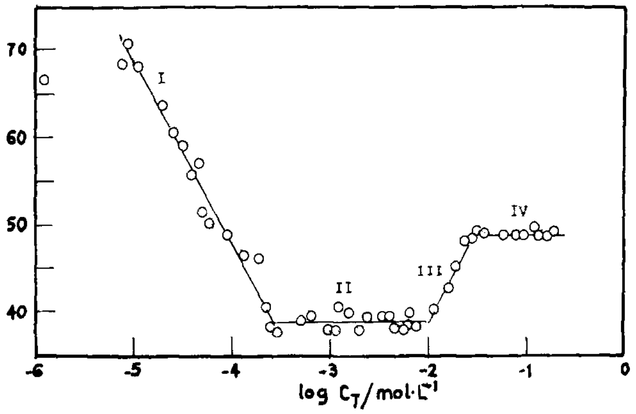

Fig. 5 Surface tension vs. the logarithm of the concentration of DTAOH. Explanations in the text

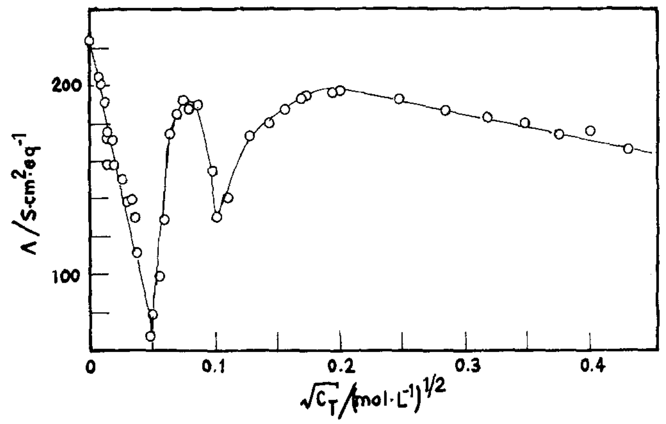

Fig. 7 Equivalent conductivity of DTAOH solutions vs. square root of the concentration

Fig. 8 Sudan III solubilization vs. the logarithm of the total concentration of DTAOH

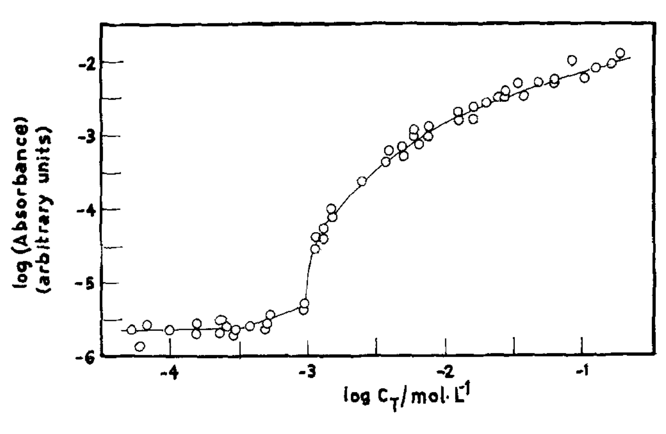

The three intersections are at $(2.78 \pm 0.69) \times 10^{-4}$ mol·dm^{-3} at $C_T = (1.06 \pm 0.45) \times 10^{-2}$ mol·dm^{-3} and $C_T = (3.1 \pm 1.2) \times 10^{-2}$ mol·dm^{-3}. This plot is very similar to Fig. 14 of the paper of Zimmels and Lin [20], who worked with sodium dodecanoate.

Conductivity measurements are shown in Figs. 6 and 7. Figure 6 shows the specific conductivity against the total concentration, and it is similar to Fig. 2 of Zimmels et al. [21]. Figure 7 shows the equivalent conductivity vs. the square root of the total concentration, this is also very similar to that obtained by Zimmels and Lin [20] with sodium octanoate and dodecanoate in water. Changes in conductivity occur at $C_T = (2.5 \pm 0.1) \times 10^{-3}$ mol·dm^{-3}, $(1.0 \pm 0.1) \times 10^{-2}$ mol·dm^{-3} and $(5.3 \pm 1.1) \times 10^{-2}$ mol·dm^{-3}.

In Fig. 8, the concentration of solubilized Sudan III (in arbitrary units) was plotted vs. C_T. The solutions below

DTAOH 2.5×10^{-4} mol·dm^{-3} are colorless. At about 3.0×10^{-4} mol·dm^{-3} a slight solubilization may be detected, which is easily noticeable at concentrations over $(1.00 \pm 0.05) \times 10^{-3}$ mol·dm^{-3}.

The use of Sudan III is not completely free of controversy, because its molecule has a phenol group which has an acid character. Since DTAOH solutions are alkaline, the phenol group may be ionized thus increasing the solubility of the dye in water. It possibly may alter the DTAOH CMC and micelle structure. This is why we also used Sudan Black B, whose molecule is neutral in alkaline solutions. Figure 9 shows the absorbance-concentration curve with this dye. The solution is colorless below 1.05×10^{-3} mol·dm^{-3}. At 5×10^{-3} mol·dm^{-3} the solubility increases very rapidly.

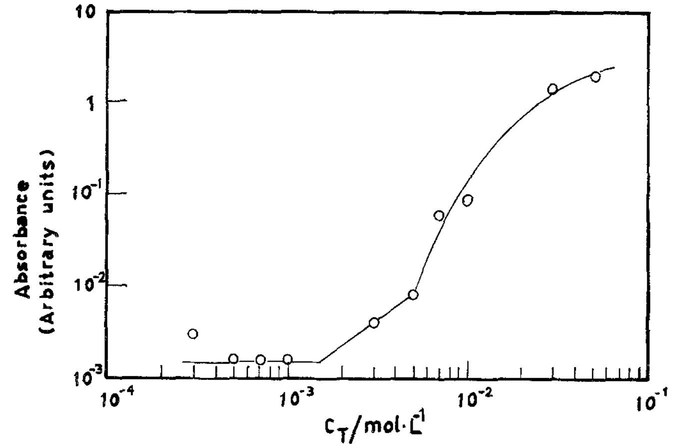

Fig. 9 Sudan Black B solubilization vs. total concentration of DTAOH

Fig. 10 Relative viscosity of DTAOH solutions vs. the total concentration

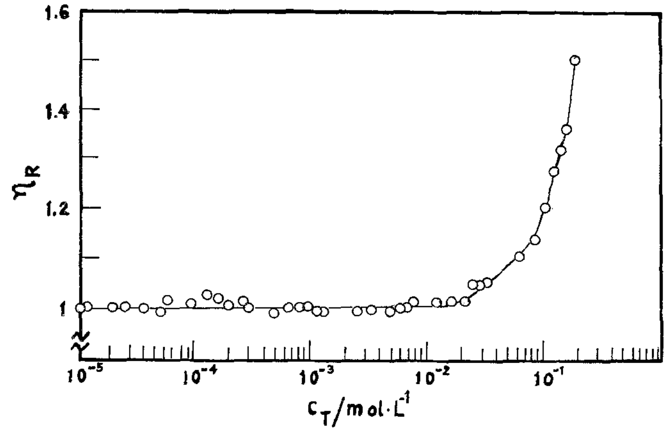

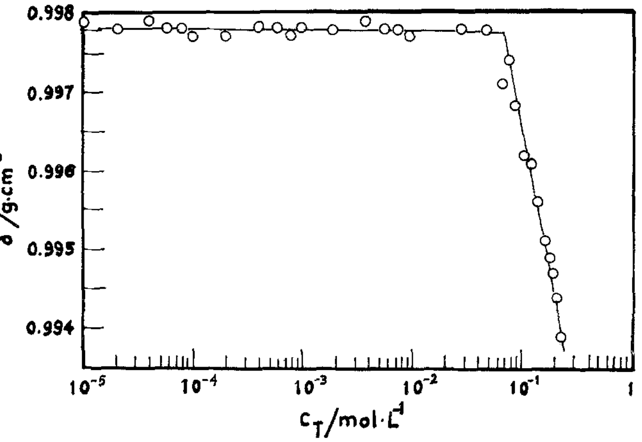

Fig. 11 Density of DTAOH solutions vs. the total concentration

Figure 10 shows the relative viscosity $\eta_R = \eta/\eta_0$ vs. the total amphiphile concentration. Here, η is the viscosity of the solution and η_0 that of the solvent (taken as that of the water). There are two different straight lines, whose equations are:

Line I:

$$\eta/\eta_0 = 0.9940 \pm 0.0011 + (0.53 \pm 0.31) C_T$$

$$r = 0.8068$$

Line II:

$$\eta/\eta_0 = 0.9759 \pm 0.0012 + (2.3879 \pm 0.0045) C_T$$

$$r = 0.9947$$

The intersection is at $(1.89 \pm 0.50) \times 10^{-2}$ mol·dm^{-3}. A second run gave similar results, with a break at $(2.8 \pm 3.4) \times 10^{-2}$ mol·dm^{-3}.

Figure 11 shows the results of density measurements with two straight lines whose equations are:

Line I:

$$\delta(g \cdot \mathrm{cm}^{-3}) = 0.99781 \pm 2.5 \times 10^{-5} - (7 \pm 19) \times 10^{-4} C_T$$

$$r = -0.8723$$

Line II:

$$\delta(g \cdot \mathrm{cm}^{-3}) = 0.998456 \pm 2.8 \times 10^{-5} - (19.56 \pm 0.19) \times 10^{-3} C_T$$

$$r = -0.9922$$

the break being at $(3.40 \pm 0.38) \times 10^{-2}$ mol·dm^{-3}

In Table 1, we summarize the CMC values from the literature and the values found in this work.

Table 1 Literature critical micelle concentration for DTAOH and DTAB aqueous solutions at 25 °C

Surfactant	CMC ($\mathrm{mol \cdot dm^{-3}}$)	Reference
LTAOH	0.0305 ± 0.0030	[4]
	0.0295 ± 0.0020	[4]
	0.00077	[4, 5]
	0.033	[50]
LTAB	0.0175	[8]
	0.011	[1]
	0.014	[1]
	0.0154	[11]
	0.0146	[12]

Critical points found in this work on LTAOH-water solutions ($\mathrm{mol \cdot dm^{-3}}$)

Method	Point a	Point b	Point c	Point d
Surface tension	2.78×10^{-4} $\pm 0.69 \times 10^{-4}$		1.06×10^{-2} $\pm 0.45 \times 10^{-2}$	3.1×10^{-2} $\pm 1.2 \times 10^{-2}$
Conductivity		2.5×10^{-3} $\pm 0.1 \times 10^{-3}$	1.0×10^{-2} $\pm 0.1 \times 10^{-2}$	5.3×10^{-2} $\pm 1.1 \times 10^{-2}$
Glass Electrode			1.20×10^{-2} $\pm 0.01 \times 10^{-2}$	
$\mathrm{DTA^+}$-ion selective electrode		1.3×10^{-3} $\pm 0.1 \times 10^{-3}$		
Solubility (Sudan III)	2.50×10^{-4}	1.00×10^{-3} $\pm 0.01 \times 10^{-3}$		
Solubility (Sudan Black B)	1.05×10^{-3}	5.0×10^{-3}		
Viscosity			1.89×10^{-2} $\pm 0.50 \times 10^{-2}$ 2.8×10^{-2} $\pm 3.4 \times 10^{-2}$	
Density				3.40×10^{-2} $\pm 0.38 \times 10^{-2}$
Average values	2.506×10^{-4} $\pm 0.099 \times 10^{-4}$	1.896×10^{-3} $\pm 0.071 \times 10^{-3}$	1.108×10^{-2} $\pm 0.010 \times 10^{-2}$	3.02×10^{-2} $\pm 0.28 \times 10^{-2}$

Discussion

Aggregation

The various results show the occurrence of phenomena related to aggregation at four different concentrations. The average values are point a: $C_T = (2.51 \pm 0.10) \times 10^{-4}$ $\mathrm{mol \cdot dm^{-3}}$, point b: $(1.300 \pm 0.041) \times 10^{-3}$ $\mathrm{mol \cdot dm^{-3}}$, point c: $C_T = (1.108 \pm 0.010) \times 10^{-2}$ $\mathrm{mol \cdot dm^{-3}}$, and point d: $(3.02 \pm 0.28) \times 10^{-2}$ $\mathrm{mol \cdot dm^{-3}}$.

Many authors have reported on systems which have multiple critical concentrations [See ref. 21 and references therein, 22–25]. In particular, there is conclusive evidence about the formation of premicellar aggregates as dimers [6, 20, 26, 27] and larger aggregates [28, 29].

Bunton et al. [9] found that hexadecyltrimethylammonium hydroxide (CTAOH) and fluoride (CTAF) systems show a large range of aggregate sizes. There are small particles at low concentrations, but their size increases with surfactant concentration until they become true micelles.

Between a and b the surface excess of amphiphile ions (Γ) is zero, which means that the surface and bulk concentration are equal and increase by the same amount [30]. This is commonly interpreted as an evidence of the existence of micelles, but it is not the only possible interpretation. It may be due to a modification of the structure of the solution affecting the activity coefficients. The results of Sudan III solubilization may indicate that some modification may occur, which affects the adsorption at the solution-air interface.

The DTA^+ ion-selective electrode, which is sensitive to single DTA^+ ions activity, indicates that the aggregation of these ions starts at point b.

The conductivity and surface tension data obtained are similar to those of Zimmels et al. [20, 21]. According to these authors, this type of behavior corresponds to a stepwise aggregation, in which point b indicates the start of premicellar aggregation, point c indicates the conventional CMC, in which the aggregates have the properties of true micelles, and point d indicates a change in micelle structure.

Bunton et al. [9] measured the specific conductivity of CTAOH vs. concentration and they found a linear relation below $C_T = 1.3 \times 10^{-3}$ mol·dm^{-3}, then the plot was curved and remained linear at concentrations above 3×10^{-3} mol·dm^{-3}. In general, the break is not well enough defined to determine accurately the intersection of the two straight lines. These authors found the CTAOH CMC = 8.6×10^{-4} mol·dm^{-3}, close to that of other CTA^+ salts. Therefore, the break in the specific conductivity vs. C_T plot found by Bunton et al. at $\simeq 1.5 \times 10^{-3}$ mol·dm^{-3} is similar to point d in DTAOH solutions, and may be due to changes in micellar structure.

The solubility data of Sudan III indicates a probable interaction between premicellar DTAOH aggregates and the dye, which has an acidic character, at $\simeq 3 \times 10^{-4}$ mol·dm^{-3}. Both dyes (Sudan III and Sudan Black B) show unequivocally micellar solubilization at point c.

The experiment with Rhodamine 6G detected micelles at concentrations larger then point c, but no micelles were detected below this concentration.

The viscosity experiments also indicate that micelles form at point c, and the glass electrode results show that at this point the counterions join the aggregates.

Many other systems (soaps, bile salts, bolaform amphiphiles) show evidence of postmicellar critical points [22–24, 31–37]. The critical point found by Lianos and Zana for DTAOH systems (3×10^{-2} mol·dm^{-3}) is close to our point d.

Micelle ionization

The values of α for RTAOH in the literature are high (0.74–0.63) [2, 3], whereas that of the corresponding bromides are 0.19–0.30 [38–41]. We found that $\alpha \simeq 0.8$ at point c, but diminishes as the surfactant concentration rises. Similar results are in the literature for RTAOH and RTAF [42, 43]. α is 0.19–0.30 for DTAB [38, 39], which confirms the assertion that RTAOH micelles are more ionized than those of RTAB. Bunton et al. [9] found $\alpha = 0.40$–0.48 for CTAOH by Evans' method, at about 1.5×10^{-3} mol·dm^{-3}, about two times the CMC. This method is probably inapplicable to RTAOH solutions, due to the high conductivity of counterions and the small, fully ionized aggregates. However, our results are not completely free of criticism: the exact nature of premicellar aggregates is not known, and this affects in an unknown amount the computation of the activity coefficients. This affects the computation of the concentration of ions from the ion-selective electrodes results. Then, both the absolute concentrations in Fig. 3 and the α values in Fig. 4 are only estimations with some uncertainty, but the general trends are probably true.

The reduction of α with the rise of the surfactant concentration is a consequence of the growth of the micelles and the increment in their concentration. The interpretation may be that the concentration increment compresses the ionic atmosphere, which is equivalent to increasing its concentration [9], or that the structure of micelles changes with the counterion concentration, affecting the counterion bonding to the micelles' Stern layer [44]. This change occurs in a wide range of concentrations with hydrophilic ions such as OH^- or F^- [42, 43], and in a narrower one with hydrophobic ions as Br^- [9].

In agreement with theories on the factors which affect micellar size and shape [45], at the CMC the DTAOH micelles must be smaller than DTAB micelles. The micelle aggregation number for DTAOH is $n = 20$ [3], and $n = 57$ for DTAB [46–49], as expected.

Since micelles are small and highly charged [2], their contribution to the total conductivity of the system must be high. The conductivity of the small micellized OH^- counterions is very high, so the real CMC is almost undetectable by conductivity measurements. At $C_T = 5.3 \times 10^{-2}$ mol·dm^{-3} a break in the specific conductivity-concentration plot is seen. It is near to the value found by Lianos and Zana (0.0305 mol·dm^{-3}) which was interpreted by these authors as the DTAOH CMC. At about the same concentration there are anomalies in the surface tension (at $C_T = 3.1 \times 10^{-2}$ mol·dm^{-3}) and density ($C_T = 3.4 \times 10^{-2}$ mol·dm^{-3}) measurements. These anomalies occur at very low α values (about 0.05). This may mean that the micelle structure changes.

Conclusions

DTAOH has a stepwise aggregation at four different concentrations. The average values are point a: $C_T = (2.51 \pm 0.10) \times 10^{-4}\,\mathrm{mol \cdot dm^{-3}}$ which is of uncertain interpretation, point b: $C_T = (1.300 \pm 0.0410) \times 10^{-3}\,\mathrm{mol \cdot dm^{-3}}$, which corresponds to the formation of small aggregates which grow with increasing concentration: point c: $C_T = (1.108 \pm 0.010) \times 10^{-2}\,\mathrm{mol \cdot dm^{-3}}$, which corresponds to the formation of true micelles (CMC) and point d: $(3.02 \pm 0.28) \times 10^{-2}\,\mathrm{mol \cdot dm^{-3}}$, in which probably the structure of micelles changes affecting their properties.

The DTAOH micelles are highly ionized ($\alpha = 0.8$) at the CMC, close to the literature values ($\alpha = 0.74$–0.68) [2, 3]. However, α decreases to reach very small values when C_T increases.

Work is in progress to elucidate the structure of micelles and premicellar aggregates.

Acknowledgements Two of us (M.A.M. and R.M.M.) have a fellowship with Consejo Nacional de Investigaciones Cientificas y Técnicas (CONICET) de la República Argentina. This work was supported by a grant of the Universidad Nacional del Sur.

References

1. de Graça Nascimento M, Miranda SAF, Nome F (1986) J Phys Chem 90:3366
2. Ortega F, Rodenas E (1987) J Phys Chem 91:837
3. Lianos P, Zana R (1983) J Phys Chem 87:1289
4. Paredes S, Sepúlveda L, Tribout M (1984) J Phys Chem 88:1871
5. Abuin EA, Lissi E, Araujo PS, Aleixo RMV, Chaimovich H, Bianchi N, Miola L, Quina FH (1983) J Colloid Interface Sci 96:293
6. Kale KM, Kussler EL, Evans DF (1982) J Soln Chem 11(8):581
7. Mukerjee P, Mysels KJ (1971) Natl Stand Ref Data Ser, Natl Bur Stand N° 36
8. Rico I, Latter A (1986) J Phys Chem 90:5970
9. Bunton C, Gan L, Moffat J, Romsted L, Savelli G (1981) J Phys Chem 85:4118
10. Klevans HB (1948) J Phys Colloid Chem 52:130
11. Evans DF, Allen M, Ninham BW, Fouch A (1984) J Soln Chem 13(2):87
12. Anacker EW, Rush RM, Johnson JS (1964) J Phys Chem 68:81
13. Davies CW (1962) Ion Association, Butterworths, London p 41
14. Schulz PC (1988/89) Colloids and Surfaces 34:69
15. Corrin ML, Harkins WD (1947) J Chem Soc 69:679
16. Sheppard SE (1942) Rev Mod Phys 14:303
17. Kortüm G (1936) Z physik Chem B33:1 – (1986) B34:255
18. Lewschin WL (1934) Acta Physicochim URSS 1:685
19. Mandel J (1964) Statistical Analysis of Experimental Data Interscience Pub Co New York
20. Zimmels Y, Lin IJ (1974) Colloid Polym Sci 252:594
21. Zimmels Y, Lin IJ, Friend JP (1975) Colloid & Polymer Sci 253:404
22. Sköld RO, Tunius MAR (1992) J Colloid Interface Sci 152(1):183
23. Danielsson I (1956) Acta Acad Abo Ser B XX(15):165
24. Meguro K, Ikeda K, Otsuji A, Taya M, Yasuda M, Esumi K (1987) J Colloid Interface Sci 118:372
25. Elworthy PH (1959) J Pharm Pharmacol 11:557
26. Mukerjee P (1965) J Phys Chem 69:2821
27. Shedlowsky L, Jacob CW, Epstein MB (1963) J Phys Chem 67:2075
28. Stenius P, Zilliacus CH (1971) Acta Chem Scand 25(6):2232
29. Stenius P (1969) Chim Phys Appl Prat Ag Surface C R Congr Inter Deterg 5th Sept 1968 09–13:1023
30. Schukin ED, Pertsov AV, Amélina EA (1988) Quimica Colloidal, MIR, Moscow p 56
31. Ekwall P (1964) Proc IVth Internat Congress on Surf Activ Subst p 651
32. Ekwall P, Lemström KE, Eikrem H, Holmberg P (1967) Acta Chem Scand 21:1402
33. Ekwall P, Danielsson I, Stenius P (1972) in M T P International Review of Science Surface Chemistry and Colloids Physical Chemistry, London Vol 7 p 97
34. Wolfram E, Boross V (1971) Forschrittsber Kolloid Polymer 55:143
35. Durand RR, Yvette W (1968) C R Acad Sci Paris, Ser C 266(25):1658
36. Muller N, Pellerin JH, Chen WW (1972) J Phys Chem 76:1 3012
37. Ödberg L (1972) J Colloid Interface Sci 41:2, 298
38. Anacker EW, Ghose HM (1963) J Phys Chem 67:1713
39. Anacker EW, Westwell AE (1964) J Phys Chem 68:3490
40. Zana R (1980) J Colloid Interface Sci 87:330
41. Lianos P, Zana R (1983) J Phys Chem 87:1289
42. Gunnarsson G, Johnsson B, Wennerstrom H (1980) J Phys Chem 84:3114
43. Rohde A, Sackmann E (1979) J Colloid Interface Sci 70:494 – (1980) J Phys Chem 84:1598
44. Bunton CA, Frankson J, Romsted IS (1980) J Phys Chem 84:2607
45. Schulz PC (1991) Colloid & Polym Sci 269:612
46. Lianos P, Zana R (1980) J Phys Chem 84:3339
47. Lianos P, Zana R (1980) Chem Phys Lett 76:62
48. Lianos P, Zana R (1981) J Colloid Interface Sci 84:100
49. Lianos P, Zana R (1981) J Colloid Interface Sci 88:594
50. Ninham BW, Evans DF, Wei GJ (1983) J Phys Chem 87:5020